ARTICLE

# Effects of Supports and Promoters on *in situ* Hydrogenation of *o*-Cresol over Ni-based Catalysts

Yan-bin Li[a,b], Ying Xu[a], Long-long Ma[a,b*], Tie-jun Wang[a], Qi Zhang[a], Guan-yi Chen[b]

*a. Key Laboratory of Renewable Energy, Guangzhou Institute of Energy Conversions, Chinese Academy of Sciences, Guangzhou 510640, China*
*b. Faculty of Environmental Science and Engineering & State Key Lab of international Combustion Engine, Tianjin University, Tianjin 300072, China*

(Dated: Received on June 1, 2014; Accepted on June 6, 2014)

We investigated the effects of supports (CMK-3, $SiO_2ZrO_2$, MgO, $Al_2O_3$) and promoters (Cu, Ce, Fe) on textual properties of Ni based catalysts. *o*-Cresol was used as a probe to test the activity of these catalysts under the condition of 230 °C and nitrogen pressure of 0.1 MPa. The catalysts were characterized by X-ray diffraction, $H_2$ temperature programmed reduction ammonium programmed desorption, and $N_2$ adsorption-desorption isotherms. The results showed that the catalytic performance of Ni/CMK-3 (the conversion of *o*-cresol reached 45.4%) was significantly better than the other three kinds of supports. The modification of Ni/CMK-3 was also investigated and over 60% conversion of *o*-cresol was obtained after the addition of Ce (64.6%)and Cu (66.8%) in Ni/CMK-3, whereas the addition of Fe led to a decrease of conversion. In the meantime, Cu changed the products distribution. The appearance of toluene indicated that another pathway existed in the reaction. Accompanied by the ascension of conversion in both sides, side effects also occurred and got more serious. The apparent order of activity for all the tested catalysts was NiCe/CMK-3> NiCu/CMK-3>Ni/CMK-3>NiFe/CMK-3>$Ni/Al_2O_3$>$Ni/SiO_2ZrO_2$>Ni/MgO. The reaction pathway, involving three routes, was also mentioned in this study.

**Key words:** *in-situ* hydrogenation, Support, Promoter, *o*-Cresol

## I. INTRODUCTION

Along with the growing price of crude oil and the concern about the greenhouse effect, the research of renewable resource attracts much attention. Bio-oil is derived from biomass, the only renewable carbon containing feedstock that can be used for the synthesis of hydrocarbon transportation fuels [1]. It is considered as an important substitute for fossil fuel, whereas bio-oil has complicate physical and chemical properties including high water content [2], high viscosity, high corrosion [3], and other serious problems. So bio-oil must be converted to higher quality fuels by refining process [4]. Among many techniques, hydrogenation has the relatively higher efficiency in traditional bio-oil refining processes. There are lots of studies on the textual properties of catalysts and the refining of bio-oil [5−9]. As phenol compounds are relatively abundant [10] and intractable [11] in bio-oil hydrogenation, they are always chosen as model compounds in hydrogenation study. In the hydroprocessing, phenols can react with $H_2$ to generate cyclohexanol, cyclohexanone or their derivatives. Cyclohexane compounds can be obtained from deep hydrogenation [12].

Traditional hydrogenation processes mainly use $H_2$ as hydrogen source directly, but external hydrogen supply has many problems in production, transportation and storage, and also utilization efficiency of $H_2$. Li *et al.* [13, 14] proposed *in situ* hydrogenation system, coupling the aqueous-phase reforming (APR) of methanol and hydrogenation process to generate $H_2$ and the hydrogenation happened simultaneously. A series of problems caused by external hydrogen supply can be avoided. In this work, we investigated the effects of different supports and promoters on Ni based catalysts and the test was carried out in the *in situ* hydrogenation reaction. Based on previous research [15], *o*-cresol was chosen as a model compound, to represent phenol compounds containing two or more groups. The textual properties of catalysts, including surface area, surface acidity, reductivity were tested. The mechanism was also discussed.

## II. EXPERIMENTS

### A. Catalysts preparation

MgO, $Al_2O_3$, $SiO_2ZrO_2$, CMK-3 were chosen as the supports of Ni based catalysts. $SiO_2ZrO_2$ and

*Author to whom correspondence should be addressed. E-mail: mall@ms.giec.ac.cn

 

CMK-3 (a kind of carbon mesoporous material) were prepared by the methods as described in Refs.[16, 17]. MgO and $Al_2O_3$ were purchased from Tianjin Fuchen chemical reagent factory. The precursors of promoters ($Cu(NO_3)_2{\cdot}6H_2O$, $Ce(NO_3)_3{\cdot}6H_2O$ and $FeCl_3$) were purchased from Guangzhou chemical reagent factory.

NiCu/CMK-3 was prepared by wet impregnating CMK-3 with $Ni(NO_3)_2{\cdot}H_2O$ and $Cu(NO_3)_2{\cdot}6H_2O$ mixed aqueous solutions. The catalysts contained 20wt% Ni and 1wt% promoter. The solution was evaporated while the residue was dried at 120 °C. The catalysts were pretreated in a continuous flow setup, where the catalysts were reduced at 550 °C in the flow of 5% hydrogen mixed with 95% nitrogen. In the same way, we obtained the catalysts of Ni/MgO, $Ni/SiO_2ZrO_2$, $Ni/Al_2O_3$, NiCe/CMK-3 and NiFe/CMK-3.

### B. Catalytic experiments

The experiment was carried out in 50 mL stainless autoclave equipped with a paddle stirrer. For each run, 0.5 g catalyst, 9 g water, 4.8 g methanol, and 1.1 g *o*-cresol were loaded into the autoclave. The air was displaced with nitrogen by repetitive evacuation and eventually the pressure was adjusted to 0.1 MPa. Then the stirrer was set to 400 r/min, and the reactions were carried out at 230 °C for 9 h. After cooling back to room temperature, gas and liquid samples were collected and analyzed in gas chromatography (GC).

### C. Catalysts characterization

Specific surface area and pore size distribution of catalysts were measured by brunauer-Emmett-Teller (BET) method, using Quantachrome-iQ-2 adsorption instrument. Liquid nitrogen adsorption method was used to test surface area. Generally, the carbon support has significantly larger surface area than the other tested supports. X-ray diffraction (XRD) patterns were recorded using a Rigaku D/max-rC with a Cu K$\alpha$ radiation source. Scan step was 0.02°, scanning in 5°−80°. All samples were analyzed as prepared powder.

The reductivity of catalysts was characterized by hydrogen temperature-programmed reduction ($H_2$-TPR). The surface acidity of Ni based catalysts was evaluated by temperature programmed desorption of ammonium ($NH_3$-TPD). The TPR test was performed in a quartz U-tube reactor with a thermal conductivity detector (TCD). For each experiment, 50 mg of catalysts was packed into U-tube reactor and pretreated under flowing helium (40 mL/min) at 400 °C and kept for 30 min, then heated in a flow of 5vol%$H_2$/95vol%$N_2$ (40 mL/min) from 50 °C to 900 °C at a rate of 10 °C/min.

In the case of TPD experiment, 50 mg of catalyst was pretreated in the flow of helium (40 mL/min) at 500 °C and kept for 60 min, then ammonia adsorption was carried out after cooling to 120 °C. Subsequently, excessive physically adsorbed ammonia was purged by purging with helium at 120 °C for 60 min. $NH_3$-TPD tests were carried out by increasing the temperature from 120 °C to 850 °C at a rate of 10 °C/min under the same flow of helium.

### D. Product analysis

Identification of liquid products was conducted by a gas chromatograph-mass spectrometry system (GC/MS, Agilent 7890N and 5973N. with HP innowax column). Quantitative analysis was performed with a GC Shimadzu GC2014 equipped with a flame ionization detector (FID) and a thermal conductivity detector (TCD). External standard method was established for the test of *o*-cresol, 2-methylcyclohexanol, 2-methylcyclohexanone and toluene, using methanol as solvent. The following equations are used to calculate conversion and selectivity of *o*-cresol and products:

$$X = 1 - \frac{W_{\rm r}}{W_{\rm i}} \times 100\% \tag{1}$$

$$S = \frac{M_{\rm one}}{M_{\rm all}} \times 100\% \tag{2}$$

where $X$ is conversion, $S$ is selectivity. $W_{\rm r}$ and $W_{\rm i}$ are the weights of residual *o*-cresol and initial *o*-cresol, respectively. $M_{\rm one}$ and $M_{\rm all}$ are the moles of one product and all products.

The hydrogenation and APR reaction both existed in the *in situ* hydrogenation reaction. In order to reflect the effect of hydrogen production, real hydrogen yield $Y$ was calculated by Eq.(3):

$$Y = 3M_{\rm CO_2} + 2M_{\rm CO} - 4M_{\rm methanol\rightarrow methane} \tag{3}$$

where $M_{\rm CO_2}$, $M_{\rm CO}$, and $M_{\rm methanol\rightarrow methane}$ are the moles of $CO_2$, CO, and the conversion of methanol to methane.

## III. RESULTS AND DISCUSSION

### A. Textual properties of catalysts

#### 1. $N_2$ adsorption-desorption of catalysts

The average pore size and specific surface area of catalysts are listed in Table I.

As shown in Table I, Ni/CMK-3 had the largest specific surface area (985.03 $m^2/g$). After the addition of promoters, the specific surface area decreased in different degree. Cu and Ce did not trigger obvious reduction, whereas promoter Fe made the surface area reduce to 783.74 $m^2/g$, pore volume increased to 0.86 cc/g. The addition of Fe probably resulted in the reduction of pore number, it made pore volume increase but surface area decrease.

DOI:10.1063/1674-0068/27/06/697-703 

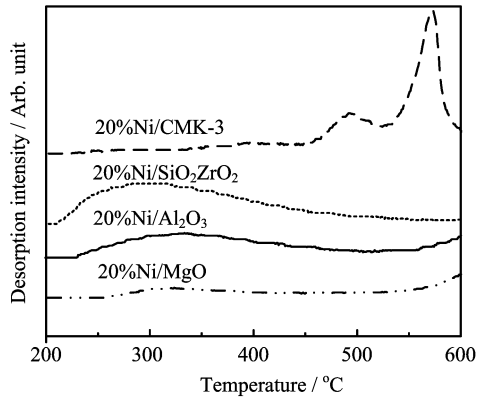


FIG. 1 $NH_3$-TPD profiles of nickel-based catalysts with different supports.

TABLE I Average pore size $d$, pore volume $V$, and specific surface area $A$ of catalysts.

| Catalyst | $A/(m^2/g)$ | $d$/nm | $V/(cc/g)$ |
|---|---|---|---|
| 20%Ni/MgO | 78.85 | 17.52 | 0.61 |
| 20%Ni/$SiO_2ZrO_2$ | 176.72 | 1.44 | 0.64 |
| 20%Ni/$Al_2O_3$ | 272.53 | 9.57 | 0.84 |
| 20%Ni/CMK-3 | 985.03 | 3.40 | 0.75 |
| NiFe/CMK-3 | 783.74 | 3.58 | 0.86 |
| NiCu/CMK-3 | 927.20 | 3.62 | 0.77 |
| NiCe/CMK-3 | 972.45 | 3.73 | 0.73 |

### 2. $NH_3$-TPD results of catalysts with different supports

The acidity of all catalysts was determined and the profiles are given in Fig.1. The area of desorption peaks revealed that the amounts of acid sites on the surface of catalysts and the temperature where the desorption peaks emerged revealed the acidic strength of catalysts. Ni/MgO belonged to basic catalyst, so the curve did not present an obvious desorption peak. Ni/$Al_2O_3$ and Ni/$SiO_2ZrO_2$ presented a moderate amount of acidic sites, which was evidenced by the broad desorption peaks around 300 °C. The desorption peak of Ni/CMK-3 was centered at 440 and 530 °C, and the former one could be attributed to stronger acid sites [18]. In contrast with other TPD profiles, the peak at 530 °C might be related to $H_2O$. The results revealed that the order of acidic strength was as follows: Ni/CMK-3 >Ni/$SiO_2ZrO_2$≈Ni/$Al_2O_3$>Ni/MgO.

### 3. X-ray diffraction of catalysts with different promoters

The X-ray diffraction patterns of all catalysts with promoters are displayed in Fig.2. Nickel showed the characteristic peaks of this polymorph at 44.51°, 51.85°, and 76.37°, which corresponded to the (111), (200), (220) reflection of graphite. Simultaneously, adding promoters made characteristic peaks weak and broad,

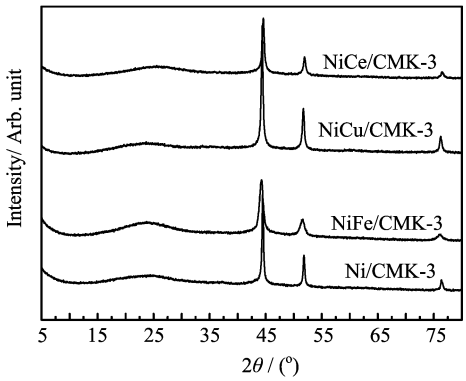


FIG. 2 XRD patterns of Ni/CMK-3 with different promoters.

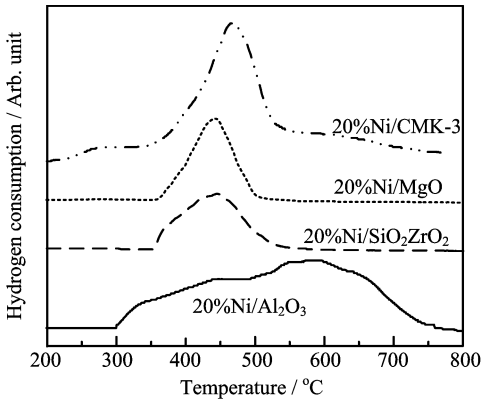


FIG. 3 $H_2$-TPR profiles of Ni based catalysts with different supports.

illustrating that adding promoters improved the Ni dispersion on supports, the dispersant effect ranked as follows: Ce>Cu>Fe.

### 4. $H_2$-TPR results of catalysts

The $H_2$-TPR profiles of Ni based catalysts with different supports are listed in Fig.3. Reduction peaks of four catalysts all appeared around 450−500 °C which were attributed to NiO. Because the peak of pure NiO was around 250−400 °C [19], the results indicated that all the studied catalysts presented significant metal-support interactions. It revealed that the dispersion of Ni increased with reduction temperature [20]. The reduction peak of Ni/CMK-3 was mainly centered at 480 °C. This indicated the existence of a majority of strongly interacting Ni species. In the case of Ni/$SiO_2ZrO_2$ and Ni/MgO, the reduction peaks were observed at 450 °C, which were relatively weaker interaction between NiO and supports than Ni/CMK-3. Ni/$Al_2O_3$ had a broad peak in the profile. These obvious hydrogen consuming peaks could be observed at 350, 460, and 600 °C. The hydrogen consuming peaks at 350 and 460 °C respectively belonged to the free

DOI:10.1063/1674-0068/27/06/697-703 

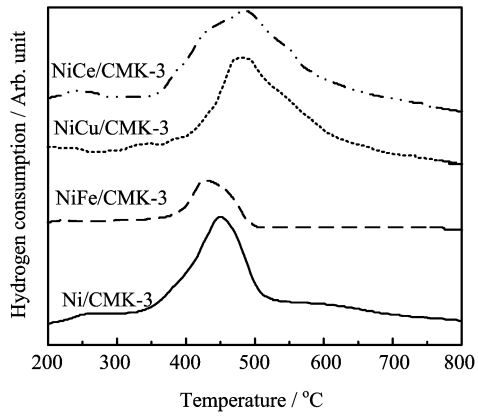


FIG. 4 $H_2$-TPR profiles of Ni/CMK-3 with promoters.

state and dispersed state of NiO [21], The $Ni^0$ particles, which reduced from free state of NiO, had weaker catalytic activity. Dispersed state of NiO can be reduced to smaller $Ni^0$ particles, which can promote the activity of catalyst [22]. The peak at 600 °C was presented by some hardly reductive species such as $NiAl_2O_4$ [23, 24].

The $H_2$-TPR profiles of Ni/CMK-3 with different promoters (shown in Fig.4) supported the conclusion obtained from the XRD patterns. Different from the former test, the main hydrogen consuming peak of Ni/CMK-3 was centered at 460 °C. For the NiCe/CMK-3 and NiCu/CMK-3, the reduction peaks were around 490 °C, which was attributed to the improvement of Ce and Cu to Ni dispersion. The reduction feature of NiFe/CMK-3 showed the hydrogen consuming peak at 440 °C, which revealed the addition of Fe did not improve the dispersion of Ni, it was likely related to the porous channel plugged by promoter. The obvious reduction of surface area of NiFe/CMK-3 also supported this inference.

### B. Catalytic activity of catalysts

#### 1. The effects of catalysts with different supports

The gas composition is shown in Fig.5. The gas composition and real $H_2$ yield mainly revealed the reaction effect and the catalyst activity in the APR reaction. The relative content of CO reached the highest point over Ni/CMK-3 in the four catalysts, whereas the ratio of CO in all carbon based gas was not more than 10%. Methane as the main side product, reached the highest points over the catalyst of $Ni/SiO_2ZrO_2$ and $Ni/Al_2O_3$, which were 68.7% and 47.6%. By contrast, the selectivity of methane was much lower in the reaction over Ni/CMK-3 (7.05%) and Ni/MgO (13.84%). The highest hydrogen yield was obtained from the reaction over Ni/CMK-3 (0.021 mol). Although the selectivity to methane consumed almost 50% $H_2$, the real hydrogen yield over $Ni/Al_2O_3$ reached 0.017 mol. The

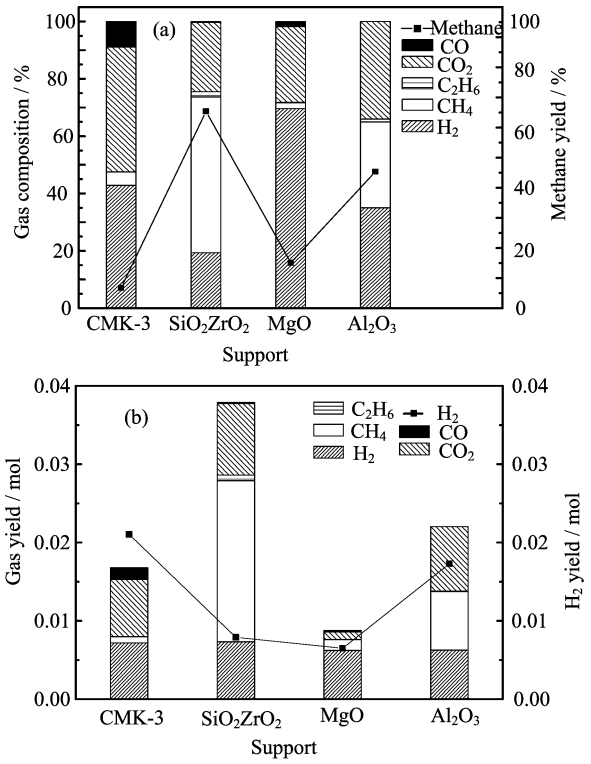


FIG. 5 (a) The composition of gas generated from *in-situ* hydrogenation, catalyzed by nickel-based catalysts with different supports. (b) The absolute amount of gas-phase products and real hydrogen yield with Ni-supported catalysts.

APR reaction over $Ni/SiO_2ZrO_2$ and Ni/MgO only generated 7.8 and 6.3 mmol $H_2$ respectively. In summary, Ni/CMK-3 exhibited the highest activity in the APR reaction from methanol, and did not cause serious side effect.

The conversion and selectivity of *o*-cresol over different supports are presented in Fig.6. As expected, both Ni/CMK-3 (45.35%) and $Ni/Al_2O_3$ (30.87%) had better catalytic behavior. The conversion of *o*-cresol over Ni/MgO and $Ni/SiO_2ZrO_2$ achieved only 6.83% and 8.19%. With regard to products distribution, selectivity to 2-methylcyclohexanol reached 89.7% in the case of $Ni/SiO_2ZrO_2$. For other catalysts, the major product was 2-methylcyclohexanone. Low selectivity of 2-methylcyclohexanol illustrated the hydrogenation of *o*-cresol was difficlut to proceed completely. But subject to the relatively selectivity of 2-methylcyclohexanol, the conversion of *o*-cresol over $Ni/SiO_2ZrO_2$ was too low.

Considering that catalytic behavior, Ni/CMK-3 exhibited better activity in APR and hydrogenation reaction. It was probably related to the high surface area, the acidity of CMK-3 and the high dispersion of Ni. Under the same reaction condition, the conversion of *o*-cresol over $Ni/Al_2O_3$ reached 30.87%, the selectivity to methane also increased to 47.6%. By contrast, $Ni/SiO_2ZrO_2$ and Ni/MgO were lack of enough catalytic activities for the coupling reaction. Over the

DOI:10.1063/1674-0068/27/06/697-703 

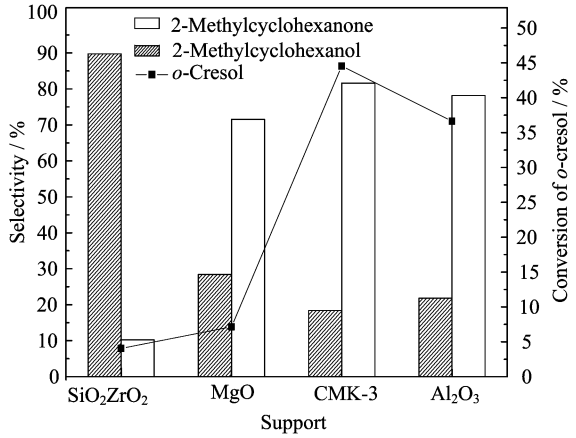


FIG. 6 Conversion and selectivity of *o*-cresol over Ni-based catalysts.

$Ni/SiO_2ZrO_2$ catalyst, 91% $H_2$ was consumed in the side reaction, whereas Ni/MgO exhibited low activity on hydrogen production and hydrogenation, which was probably related to its low surface area and the basicity of MgO support. To sum up, the Ni/CMK-3 was the best catalyst because of the highest conversion of *o*-cresol and methanol.

## 2. The effect of catalysts with different promoters

Ni/CMK-3 was modified with different promoters (Ce, Cu, Fe) to investigate the effects of *in situ* hydrogenation. The results are shown in Fig.7.

From Fig.7, the selectivity to methane over NiCe/CMK-3 (28.2%) and NiCu/CMK-3 (56.8%) obviously increased, whereas the selectivity over NiFe/CMK-3 decreased from 8.35% to 7.04%. The reduction of the CO relative content indicated that the addition of promoters was probably beneficial to the water gas shift reaction [25]. As shown in Fig.7(b), Ce promoter improved the real hydrogen yield in the coupling reaction, whereas Cu and Fe led to the reduction of $H_2$ yield.

In the experiments with modified Ni/CMK-3 catalysts, higher conversion was observed compared to the catalysts mentioned above. Figure 8 summarized the conversion and selectivity of products over Ni/CMK-3 with different promoters. With the addition of Cu, the conversion of *o*-cresol achieved 66.81%, relative to 64.59% and 40.94% over the Ce and Fe promoter. For the selectivity of products, the selectivity over NiCe/CMK-3 was similar to Ni/CMK-3. NiFe/CMK-3 performed the best with the highest selectivity of 2-methylcyclohexanol (90.85%), indicating the hydrogenation reaction over NiFe/CMK-3 proceeded much more completely. The selectivity to toluene over NiCu/CMK-3 reached 37.18%, indicating that the hydrogenolysis of *o*-cresol was accelerated in the presence

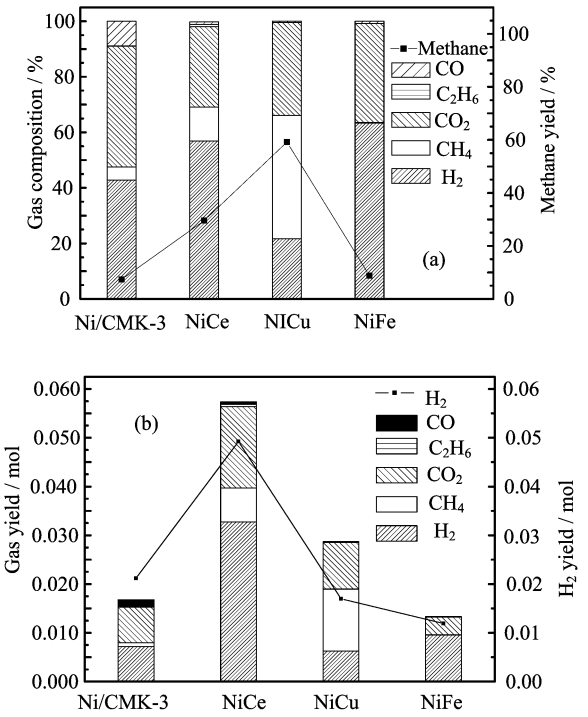


FIG. 7 (a) The composition of gas phase products over Ni/CMK-3 catalysts with different promoters. (b) Absolute amount of gas phase products and real hydrogen yield over Ni/CMK-3 with different promoters.

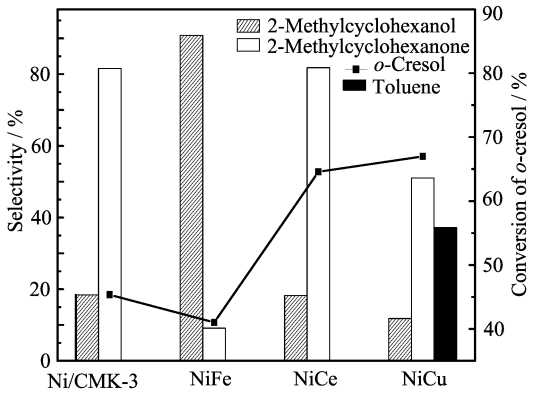


FIG. 8 Conversion and selectivity of products with Ni/CMK-3 adding different promoters.

of Cu. Ausavasukhi *et al.* [26] investigated gallium-modified beta zeolite catalysts for hydrodeoxygenation of *m*-cresol, it was mentioned that the absence of $H_2$ made the activity of hydrogenolysis and deoxygenation rapidly deplete, which can probably explain the lack of toluene and the low yield of 2-methyl cyclohexanol in the *in situ* hydrogenation.

The mechanism of hydrogenation from *o*-cresol to toluene is shown in Fig.9. The formation of toluene was also related to the adsorption sites between *o*-cresol and catalyst surface [27]: when the coplanar adsorption between the benzene ring and the cata-

DOI:10.1063/1674-0068/27/06/697-703 

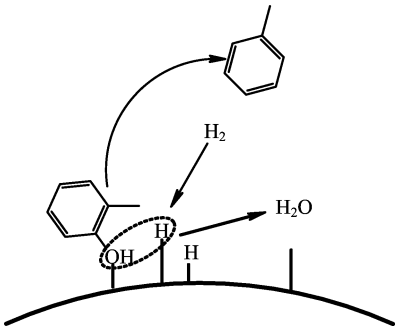


FIG. 9 The mechanism of hydrogenation from *o*-cresol to toluene.

lyst surface happens, 2-methylcyclohexanone and 2-methylcyclohexanol will generate from *o*-cresol. If the hydroxyl group is adsorbed on the surface of catalyst from the vertical direction, it will lead to the formation of toluene.

Selectivity of toluene exists a confirmed tendency (*p*-cresol>*o*-cresol>*m*-cresol [28, 29]). The utilization of hydrogen in liquid phase could be improved when the solvent was replaced from water to *n*-heptane [30], which can make the selectivity of toluene decrease. Solvent polarity, $H_2$ surface coverage and adsorption of cresol may also affect the selectivity of toluene.

Considering that real hydrogen yield, side effect, the conversion of *o*-cresol and other parameters, the best result was obtained from the reaction over NiCe/CMK-3: real hydrogen yield was 0.049 mol, the conversion of *o*-cresol reached 64.6%.

### C. Mechanism of the reaction

According to recent reports of phenols (cresol/guaiacol/phenol) hydrogenation and analysis of gas/liquid products in this experiment [26, 30−33], the possible pathway consists of three routes: (i) Direct hydrogenation of GUA's benzene ring to 2-methylcyclohexanone and 2-methylcyclohexanol. (ii) Hydrogenolysis of *o*-cresol to toluene. (iii) Interaction between some *o*-cresol molecules, they will generate slowly to 2,5-dimethyl cyclohexanol and phenol. Different from guaiacol, methyl in *o*-cresol is not easily detached from benzene rings. The reaction mechanism is shown in Fig.10. As an electron donating group, methyl can't be easily removed compared to methoxy. So the phenols [33−35] are difficult to be generated from cresol. The selectivity of 2-methylcyclohexanol is also lower than phenol and guaiacol.

## IV. CONCLUSION

In the present work, a series of catalysts were tested and modified to investigate their activities and coupling effects. The catalysts were characterized by XRD, $H_2$-TPR, $NH_3$-TPD, and $N_2$ adsorption-desorption isotherms.

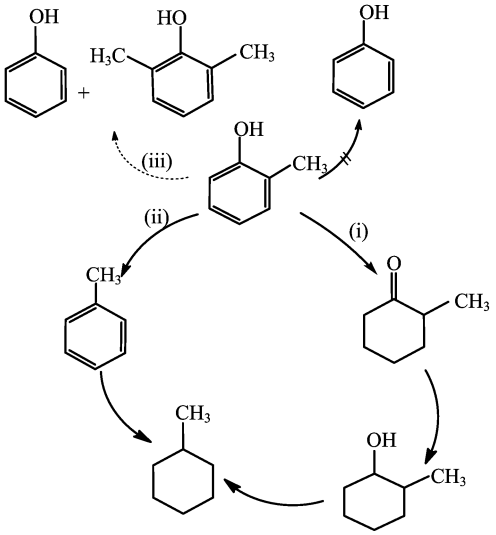


FIG. 10 Reaction mechanism analysis of *o*-cresol.

Under the given condition, Ni/CMK-3 had better coupling effect compared to other Ni based catalysts. The conversion of *o*-cresol (45.35%) and real hydrogen yield (0.021 mol) reached the highest point. The combination of good Ni dispersion, stronger acid sites, and high surface area probably led to better catalytic behavior.

For a series of catalysts modified in the catalytic activity, the addition of Cu (66.8%) and Ce (64.6%) in Ni/CMK-3 could promote the conversion of *o*-cresol greatly, because promoter Cu and Ce improved Ni dispersion in supports surface. Side effects also got more serious accompanied by ascension of conversion. In the APR reaction, Ce as a good addition can increase real hydrogen yield from 0.021 mol to 0.049 mol. Reaction pathway, involving three routes, was also mentioned: direct hydrogenation, hydrogenolysis, and interaction between some *o*-cresol molecules. It explained the difference of product distribution over these catalysts.

## V. ACKNOWLEDGMENTS

This work was supported by the National Natural Science Foundation of China (No.51036006 and No.51106108) and the Key Program of the Chinese Academy of Sciences (No.KGZD-EW-304-3).

[1] L. R. Lynd, J. H. Cushman, R. J. Nichols, and C. E. Wyman, Science **251**, 1318 (1991).

DOI:10.1063/1674-0068/27/06/697-703 

[2] B. Scholze and D. Meier, J. Anal. Appl. Pyrolysis **60**, 41 (2001).
[3] C. A. Fisk, T. Morgan, Y. Ji, M. Crocker, C. Crofcheck, and S. A. Lewis, Appl. Catal. A **358**, 150 (2009).
[4] T. R. Brown, R. Thilakaratne, R. C. Brown, and G. Hu, Fuel **106**, 463 (2013).
[5] P. E. Boahene, K. K. Soni, A. K. Dalai, and J. Adjaye, Catal. Today **207**, 101 (2013).
[6] D. C. Elliott, G. G. Neuenschwander, and T. R. Hart, Acs Sustainable Chemistry & Engineering **1**, 389 (2013).
[7] J. Guo, R. Ruan, and Y. Zhang, Ind. Eng. Chem. Res. **51**, 6599 (2012).
[8] Y. Tang, W. Yu, L. Mo, H. Lou, and X. Zheng, Energy Fuels **22**, 3484 (2008).
[9] T.Prasomsri, T. Nimmanwudipong, and Y. Román-Leshkov, Energy Environ. Sci. **6**, 1732 (2013).
[10] E. Furimsky, Appl. Catal. A **199**, 147 (2000).
[11] M. S. A. Moraes, M. V. Migliorini, F. C. Damasceno, F. Georges, S. Almeida, C. A. Zini, R. A. Jacques, and E. B. Caramao, J. Anal. Appl. Pyrolysis **98**, 51 (2012).
[12] B. Yoosuk, D. Tumnantong, and P. Prasassarakich, Fuel **91**, 246 (2012).
[13] Y. Xiang, L. Kong, P. Xie, T. Xu, J. Wang, and X. Li, Ind. Eng. Chem. Res. **53**, 2197 (2014).
[14] Y. Xiang, X. Li, C. Lu, L. Ma, J. Yuan, and F. Feng, Ind. Eng. Chem. Res. **50**, **3139** (2011).
[15] Y.Yuxiao, X. Ying, W. Tiejun, M. Longlong, Z. Qi, Z. Xinghua, and Z. Xue, J. Fuel Chem. Technol. **41**, 443 (2013).
[16] X. Zhang, Q. Zhang, L. Chen, Y. Xu, T. Wang, and L. Ma, J. Chin. Catal. **35**, 302 (2014).
[17] S. Jun, S. H. Joo, R. Ryoo, M. Kruk, M. Jaroniec, Z. Liu, T. Ohsuna, and O. Terasaki, J. Am. Chem. Soc. **122**, 10712 (2000).
[18] Y. Yang, C. Ochoa-Hernández, V. A. de la Peña O'Shea, P. Pizarro, J. M. Coronado, and D. P. Serrano, Appl. Catal. B **145**, 91 (2014).
[19] N. Lin, J. Y. Yang, Z. Y. Wu, H. J. Wang, and J. H Zhu, Microporous Mesoporous Mater. **139**, 130 (2011).
[20] B. Roy, K. Loganathan, H. N. Pham, A. K. Datye, and C. A. Leclerc, Int. J. Hydrogen Energy **35**, 11700 (2010).
[21] Y. Xu, T. Wang, L. Ma, Q. Zhang, and W. Liang, Appl. Energy **87**, 2886 (2010).
[22] X. Zhang, T. Wang, L. Ma, Q. Zhang, and T. Jiang, Bioresour. Technol. **127**, 306 (2013).
[23] J. Ashok, G. Raju, P. S. Reddy, M. Subrahmanyam, and A. Venugopal, J. Nat. Gas Chem. **17**, 113 (2008).
[24] Z. Hou and T. Yashima, Appl. Catal. A **261**, 205 (2004).
[25] Y. F. Ma, G. Q. Guan, C. Shi, A. M. Zhu, X. G. Hao, Z. D. Wang, K. Kusakabe, and A. Abudula, Int. J. Hydrogen Energy **39**, 258 (2014).
[26] A. Ausavasukhi, Y. Huang, A. T. To, T. Sooknoi, and D. E. Resasco, J. Catal. **290**, 90 (2012).
[27] H. Wan, R. V. Chaudhari, and B. Subramaniam, Top. Catal. **55**, 129 (2012).
[28] S. Eijsbouts, Appl. Catal. A **158**, 53 (1997).
[29] J. Horáček, G Šťávová, V. Kelbichová, and D. Kubička, Catal. Today **204**, 38 (2013).
[30] H. Wan, R. V. Chaudhari, and B. Subramaniam, Energy Fuels **27**, 487 (2013).
[31] N. Mahata and V. Vishwanathan, J. Mol. Catal. A **120**, 267 (1997).
[32] M. S. Zanuttini, C. D. Lago, C. A. Querini, and M. A. Peralta, Catal. Today **213**, 9 (2013).
[33] H. Y. Zhao, D. Li, P. Bui, and S. T. Oyama, Appl. Catal. A **391**, 305 (2011).
[34] A. Gutierrez, R. K. Kaila, M. L. Honkela, R. Slioor, and A. O. I. Krause, Catal. Today **147**, 239 (2009).
[35] Y. C. Lin, C. L. Li, H. P. Wan, H. T. Lee, and C. F. Liu, Energy Fuels **25**, 890 (2011).

DOI:10.1063/1674-0068/27/06/697-703 